Frequency-resolved photon-electronic spectroscopy for excited state population detection

LONG XU[1], HUI DONG[2,3], AND LIBIN FU[2,4]

[1]Institute of Applied Physics and Computational Mathematics, Beijing 100088, China
[2]Graduate School of China Academy of Engineering Physics, No. 10 Xibeiwang East Road, Haidian District, Beijing, 100193, China
[3]e-mail: hdong@gscaep.ac.cn
[4]e-mail: lbfu@gscaep.ac.cn

Atomic excitation to excited states in strong laser field is the key to high-order harmonic generation below ionization threshold, yet remains unclear mainly due to the lack of proper detection methods. We propose a frequency-resolved photon-electron spectroscopy technique to reconstruct population of excited states with the second delayed laser pulse. The technique utilizes Fourier transformation to separate ionization from different excited states to different positions on the spectrum. With the advantage of separation, we provide a scheme to reconstruct populations on different excited states after the first pulse. The scheme is validated by high-precision population reconstruction of helium and hydrogen atoms. © 2018 Optical Society of America

The interaction of an intense laser field with atoms has led to many interesting phenomena, such as photoionization [1–6], high-order harmonic generation (HHG) [7–9], and frustrated ionization [10–12]. Based on the three-step model [2], strong field approximation (SFA) can profoundly understand the physical processes that include above-threshold ionization [13, 14], cutoff region of HHG [15], and high-energy plateau in the photoelectron spectra [16–19]. However, since SFA neglects the effects of excited states, it can't describe the phenomena that involve excited states, such as Freeman resonance [20], multiphoton Rabi oscillations [21], below-threshold harmonics (BTHs) [22], and the creation of Rydberg states [23]. The mechanism of BTHs has been studied with techniques such as sum frequency generation optical gating [24] in addition to being extensively modeled [25, 26], but the role of excited state has yet to be fully examined with energy resolution. Additionally, the observation on the effect of excited state by means of observing momentum distributions is now becoming available [27, 28], with the development of laser technology and pump-probe spectroscopy. Recently, in the experiment, the angular momentum component of neon atom is resolved from the photoelectron momentum distribution by the pump-probe spectroscopy [29]. Moreover, the coherent dynamics of superposition of two states in hydrogen atom [30] and molecule H_2^+ [31] are studied by theories.

On the experimental side, measurement methods of population on excited states are developing. In the early days, de Boer and Muller [11] used a long pulse (nanosecond probe pulse) to ionize the excited atoms and guarantee different energy peaks in energy distributions derive from different excited states. Then, the population can be obtained by calculating the area probability of each peak. For the metastable state, due to its long lived property, it can be detected at the microchannel plate detector (MCP) after a long flight [10, 23, 32]. In addition to the previous diligent effort to measure population on excited states, we propose a frequency-resolved photon-electron (FRPE) spectroscopy, which is an analogy of two-dimensional Fourier spectroscopy [33–37] where two dimensions are all optical frequencies without the information about photoelectron momentum distribution as we have here. In the FRPE spectroscopy, one dimension is the photoelectron momentum distribution and the other is the optical frequency. Note that the idea of FRPE is similar to some pump probe photoelectron spectroscopy [38, 39], in which the delay time between pump and probe pulses are transformed to the frequency domain. And the Fourier transform with respect to delay time has been demonstrated [40]. With measured FRPE spectra of ejected electrons, we can reconstruct the population on excited state with a good precision.

As a proof-of-principle study, we design a simple experimental scheme with two subsequent laser pulses delayed by a time interval T_d, which is defined as the time interval between the end of the first pulse and the beginning of the second pulse. The configuration is illustrated in Fig. 1(a). The first pulse is used as a pump to prepare the superposition of bound and continuum states after the atoms or molecules interact with laser field, while the second pulse, as a probing measurement, needs to be long enough to completely ionize the electrons. A detector is set to measure the momentum distribution of the electrons. At the overall interaction ends, we can obtain the final momentum distribution $F(p, T_d)$ by tuning the delay time T_d. In order to distillate the information carried by momentum distribution, we apply Fourier transform to obtain a momentum-frequency correlation spectrum $G(p, \Omega) = (2\pi)^{-1} \int F(p, T_d) \exp(-i\Omega T_d) dT_d$. To demonstrate
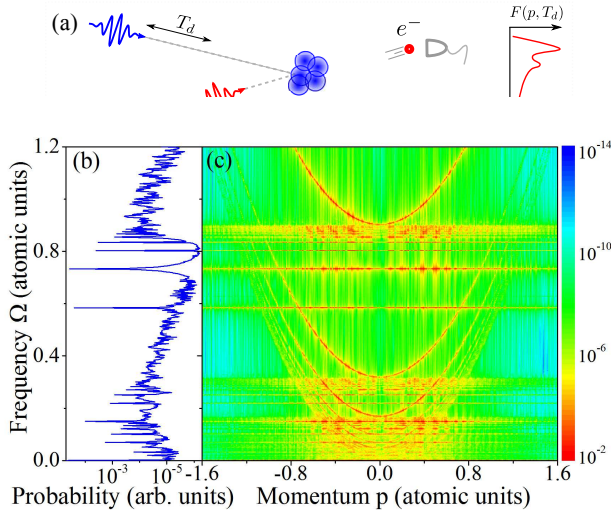
Fig. 1. (Color online) (a) Scheme of the simple 2-pulse frequency-resolved photon-electron spectroscopy. The pulse 1 (in red) prepares the initial state of atoms and the pulse 2 (in blue) is used to probe the prepared state by detecting the momentum distributions of the ejected electrons. The measurement of momentum distributions $F(p, T_d)$ is repeated with varying delay time T_d. The Fourier transformation is performed for measured spectrum $F(p, T_d)$ along T_d axis to obtain the final FRPE spectrum $|G(p, \Omega)|$. A typical spectrum with Helium as the sample is shown in subfigure (c), along with the projection to the Ω axis by integration over the electron momentum p, namely $\int dp |G(p, \Omega)|^2$, is illustrated in (b).

the advantage of the current spectroscopic method, we will numerically calculate the FRPE and show the explicit scheme to reconstruct the population on bound states, along with the population obtained by direct calculation.

Taking helium as a sample, we show the first FRPE spectroscopy in Fig. 1 (c) and the corresponding projection to Ω-axis in Fig. 1 (b). In the simulation, the ground state is selected as the initial state and the intensities of the two pulses are 10^{15}W/cm^2. We choose 150nm laser pulse with an optical cycle and 800nm laser pulse with 64 cycles as the first and second pulses, respectively. The specific form of laser field is given by $E(t) = -\partial_t A(t)$ with vector potential $A(t) = E_0/\omega \sin^2(\pi t/\tau)\cos(\omega t)$, where E_0 is the electric-field amplitude of the laser pulse with duration τ and central frequency ω. In the simulation, we obtain each slice of data $F(p, T_d)$ by solving the time-dependent Schrödinger equation of a single active electron (in atomic units)

$$i\frac{\partial}{\partial t}\Psi(x,t) = [-\frac{1}{2}\frac{\partial^2}{\partial x^2} - \frac{1}{\sqrt{x^2 + a^2}} + xE(t, T_d)]\Psi(x,t), \quad (1)$$

with fixed T_d and accumulate the full data set by scanning T_d. The second term in the right hand represents soft-Coulomb potential between electron and nucleus, where soft-core parameter [41] is chosen as $a^2 = 0.484$ for the singly charged helium.

To obtain the momentum distribution $F(p, T_d)$, we employ split-operator method [42] to numerically solve the Schrödinger equation and split the space into the inner ($|x| < x_c$) and outer

($|x| \geq x_c$) regions with x_c=800 a.u. by a smooth split function

$$F(x_c) = \begin{cases} 0, & \text{if } |x| < x_c - x_b, \\ 1, & \text{if } |x| \geq x_c, \\ \cos^4[\frac{\pi(x-x_c)}{2x_b}], & \text{otherwise,} \end{cases} \quad (2)$$

where we set the width of crossover region x_b=50 a.u.. The wave function in the inner region $\Psi(x, t)[1 - F(x_c)]$ is propagated under the full Hamiltonian numerically, while the wave function in the outer region $\Psi(x, t)F(x_c)$ is propagated under the Volkov Hamiltonian analytically [43]. In the calculation, N = 8192 grid points with a spatial step of 0.25 a.u. and the time step of 0.025 a.u. are used. The convergence is checked by comparing with the results of the more grid points, i.e., the smaller spatial and temporal step. Note that the selection of the spatial cutoff parameter x_c is primarily determined by the amplitude of free electrons in the alternating electric field $\alpha = E_0/\omega^2$ and the convergence of xc has been confirmed numerically. Here, we have chosen time delay from $T_d = 1000$ a.u. to $T_d = 4530$ a.u. with 2048 interval points. The large delay time $T_d > 1000$ a.u. ensures enough free evolution time after the first pulse. The Fourier transformation is performed after the simulation. Clearly, the spectrum shows two pronounced structures: (1) the horizontal lines at frequencies $\Omega = $ const, with constants match the energy gap between two bound states, (2) the parabolic curves $\Omega = p^2/2 + $ const. Besides, the structures of the horizontal lines $\Omega = $ const can also be seen from the result of frequency distribution given by integrating the FRPE spectrum over the momentum. We will show the physical origin of the two features in the following discussion.
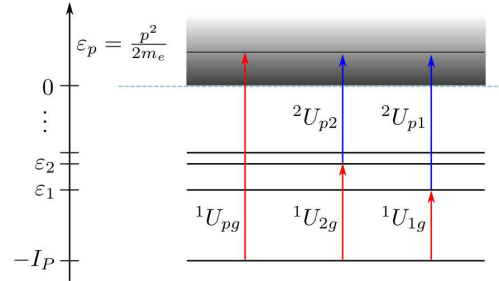

Fig. 2. Ionization diagram from the perspective of energy level transitions. g and p depict the ground and continuum states, respectively, while ε_j labels the energy of j-th excited state. ^1U and ^2U represent the entire system's evolutionary operator in the presence of the first and second laser pulses, respectively.

To understand the physical origin of the two features in the FRPE spectroscopy, we consider the evolution process from the perspective of energy level transitions. The atomic energy level diagram is illustrated in Fig. 2, with bound states $\{|e_j\rangle\}$($j = 0, 1, 2, ...$) and the continuum states $|p\rangle$. Here p is the momentum of the ionized electron. The corresponding energy of the bound state $|e_j\rangle$ is denoted as ε_j. After the first pulse, the state of the system is $|\Psi_1\rangle = {}^1U|\Psi_0\rangle$, where $|\Psi_0\rangle = |g\rangle$ is the ground state and ^1U is the evolution operator of the first pulse. In an explicit way, such state is written as $|\Psi_1\rangle = \sum_j {}^1U_{jg}|e_j\rangle + \int dp {}^1U_{pg}|p\rangle$, where $^1U_{jg} = \langle e_j|^1U|g\rangle$ and $^1U_{pg} = \langle p|^1U|g\rangle$ are the probability amplitude. The free evolution of atom

during the delay time T_d induces a phase to all the states as $|\Psi_1(T_d)\rangle = \sum_j {}^1 U_{jg} e^{-i\varepsilon_j T_d} |e_j\rangle + \int dp^1 U_{pg} e^{-ip^2/2\, T_d} |p\rangle$. After the second pulse, the wave function $|\Psi_2\rangle = {}^2 U |\Psi_1(T_d)\rangle$ takes the form

$$|\Psi_2\rangle = ... + \int dp (\sum_j {}^2 U_{pj}{}^1 U_{jg} e^{-i\varepsilon_j T_d} + {}^1 U_{pg} e^{-i\frac{p^2}{2} T_d}) |p\rangle, \quad (3)$$

where ${}^2 U_{pj} = \langle p|^2 U|e_j\rangle$ represents evolutionary operator's matrix element of the whole system when atom interacts with the second laser pulse. To get Eq. (3), we have chosen a sufficiently long T_d to ensure that the ionized electrons obtained by the first laser pulse will not be affected by the second pulse. With Eq. (3), the amplitude of electrons in particular momentum state is

$$F(p, T_d) = \left| \sum_j {}^2 U_{pj}{}^1 U_{jg} e^{-i\varepsilon_j T_d} + {}^1 U_{pg} e^{-i\frac{p^2}{2}\, T_d} \right|^2$$

$$= \sum_j \sum_m |{}^j\Lambda_{pg}||^m\Lambda_{pg}| e^{i(\theta_j - \theta_m)} e^{-i(\varepsilon_j - \varepsilon_m)T_d} + |{}^1 U_{pg}|^2 \quad (4)$$

$$+ \sum_j \left[{}^j\Lambda_{pg}{}^1 U_{pg}^* e^{-i(\varepsilon_j - \frac{p^2}{2})T_d} + {}^j\Lambda_{pg}^*{}^1 U_{pg} e^{i(\varepsilon_j - \frac{p^2}{2})T_d} \right],$$

where ${}^j\Lambda_{pg} \equiv {}^2 U_{pj}{}^1 U_{jg} = |{}^j\Lambda_{pg}| \exp(i\theta_j)$. The Fourier transform leads to the spectrum in the frequency domain as

$$G(p, \Omega) = \sum_j \sum_m |{}^j\Lambda_{pg}||^m\Lambda_{pg}| e^{i(\theta_j - \theta_m)} \delta[\Omega - (\varepsilon_m - \varepsilon_j)]$$

$$+ |{}^1 U_{pg}|^2 \delta(\Omega) + \sum_j \left[{}^j\Lambda_{pg}{}^1 U_{pg}^* \delta[\Omega + (\varepsilon_j - \frac{p^2}{2})] \right. \quad (5)$$

$$\left. + {}^j\Lambda_{pg}^*{}^1 U_{pg} \delta[\Omega - (\varepsilon_j - \frac{p^2}{2})] \right].$$

The first line of the above formula represents the bright lines $\Omega = \varepsilon_j - \varepsilon_m$ in the FRPE spectroscopy, while the second and third lines show parabolic curve $\Omega = \pm(\varepsilon_j - p^2/2)$. The current theoretical derivation shows the physical correspondence of the two main features in the Fig. 1 (c).

The separation of different processes in the spectrum provides advantages to extract further information of the ionization process. One application is to reconstruct the population on the bound states. With the advantage of labeling with energy difference $\Omega_{jm} = |\varepsilon_j - \varepsilon_m|$ on the spectrum, we can get each value $|{}^j\Lambda_{pg}||^m\Lambda_{pg}|$ at $\Omega_{jm} = |\varepsilon_j - \varepsilon_m|$ $(j \neq m)$ as $|G(p, \Omega_{jm})|$. If there are n intermediate states, we can get C_n^2 equations resulted from the interference between every two intermediate states. In other words, as long as $C_n^2 \geq n$, namely, $n \geq 3$, we arrive at the modulus $|{}^j\Lambda_{pg}|$. So we can get modules $|{}^j\Lambda_{pg}|$ by choosing three intermediate states and solving simultaneous equations. Even if there are only two intermediate states (j and m), we can solve the equations $|{}^j\Lambda_{pg}||^m\Lambda_{pg}| = |G(p, \Omega_{jm})|$ and $|{}^j\Lambda_{pg}|^2 + |^m\Lambda_{pg}|^2 = |G(p, \Omega = 0)|$. For the long pulse limit to ionizing all the electrons on the bound state $|e_j\rangle$ via the second pulse, namely, $\int |^2 U_{pj}|^2 dp = 1$, we can get the population on the bound state $|e_j\rangle$ as

$$|{}^1 U_{jg}|^2 = \int |{}^j\Lambda_{pg}|^2 dp. \quad (6)$$

Table 1. Comparison between average results obtained from the method of reconstruction with the actual value. The reconstructed values are obtained via the reconstructed scheme. The exact values are given by numerically solving Eq. (1) for the first pulse.

Population / Samples	States		ground	first excited	second excited	third excited
He	150nm 1cycle	Method(%)	63.58	11.88	15.17	1.944
		Exact(%)	63.42	11.55	15.58	1.911
		Relative Error(%)	0.2470	2.904	2.627	1.727
	100nm 2cycles	Method(%)	45.93	40.56	7.450	0.3070
		Exact(%)	45.94	38.96	7.418	0.2892
		Relative Error(%)	0.03193	4.108	0.4269	6.270
H	150nm 1cycle	Method(%)	31.82	54.39	3.578	2.291
		Exact(%)	31.50	53.15	4.407	2.886
		Relative Error(%)	1.028	2.329	18.83	20.63
	100nm 2cycles	Method(%)	67.66	23.40	0.2840	3.231
		Exact(%)	67.22	22.66	0.2840	3.769
		Relative Error(%)	0.6643	3.257	0.00128	14.26

With the reconstructed scheme, we compare the reconstructed populations on different bound states with the actual populations at the end of the first pulse from the exact numerical calculation. The details of the comparison are shown in Table 1 for both helium and hydrogen where the soft-core parameter in Eq. (1) is chosen as $a^2 = 2$ for the singly charged hydrogen. Table 1 shows the populations of four bound states for a total of four samples including two atoms and two laser pulses. Here we only choose 4 lowest levels as an example, the distribution of the remaining populations is mainly in the continuum states and partly in higher lying bound states. Owing to the property of Discrete Fourier Transform, the frequency gap after Fourier Transform is $\Delta\Omega = 2\pi/(N\triangle T_d) = 2\pi/(4530 - 1000) = 0.00178$ a.u., where N and $\triangle T_d$ represent the number of sampling points and sampling interval, respectively. Additionally, the results of reconstruction are the average of $C_4^3 = 4$ situations because we can solve the populations for every three states. In the simulation, we do not consider any decay of the bound states, noticing that the lifetime (10^{-9}s) of excited states in atoms and molecules is far longer than the time scale of the current scheme (10^{-13}s). From the table, we know that all the results of more populations are accurate, where most of the relative errors are below 5%. Moreover, the reconstruction of hydrogen is not as accurate as helium. The only reason is the ionization potential of H ($I_P = 0.5a.u.$) is smaller than He ($I_P = 0.9a.u.$), leading to less effective points $I_P/\Delta\Omega$ in the range of the ionization potential.

In view of the deviation of the result, we further study its accuracy. Taking the first sample as an example, namely, helium atom exposed to a 150nm laser pulse with 1 optical cycle, we plot the reconstructed populations in Fig. 3 (a) where the modulus $|G(p, \Omega_{jm})|$ is chosen as the maximum value in the neighbor of $\Omega_{jm} = |\varepsilon_j - \varepsilon_m|$. Obviously, the populations of $\Delta\Omega = 0.00178$ a.u. are more concentrated around the actual value than $\Delta\Omega = 0.00712$ a.u., whereas the results of $\Delta\Omega = 0.00356$ a.u. are spread out, as shown in Fig. 3 (a). This is entirely due to the fact that the function $\delta[\Omega - (\varepsilon_m - \varepsilon_j)]$ is discrete rather than continuous. Additionally, taking the area of the $|G(p, \Omega)|^2$ instead of

a point, we reselect $\left|G(p, \Omega_{jm})\right|$ as the 0.5th power of the sum of the square of a left point and a right point of Ω_{jm}, that is, $\left|G(p, \Omega_{jm})\right| = \sqrt{\left|G(p, \Omega_{jm\text{left}})\right|^2 + \left|G(p, \Omega_{jm\text{right}})\right|^2}$. The corresponding reconstructed populations are plotted in Fig. 3 (b). Compared with the results of Fig. 3 (a), the populations are more concentrated around the average values. More importantly, the accuracy is getting better with the decreasing $\Delta\Omega$. Consequently, it's indeed an effective way to improve accuracy by increasing the effective delay time length to reduce the frequency gap $\Delta\Omega$.
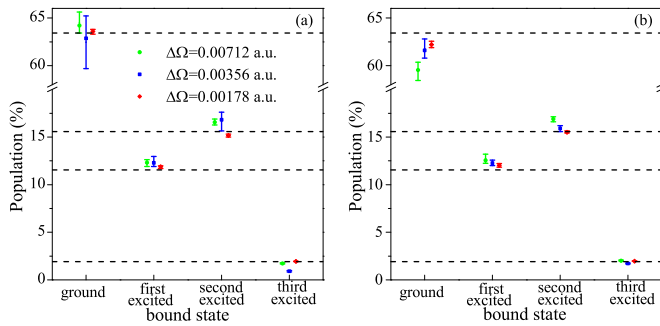

Fig. 3. The reconstructed populations of the first sample for three different frequency gap $\Delta\Omega$, 0.00712 (green), 0.00356 (blue), 0.00178 (red) a.u.. The points represent the average values, while the error bar represents the maximum and minimum values. The dashed lines depict the exact values given by numerically solving Eq. (1). The modulus $\left|G(p, \Omega_{jm})\right|$ is chosen as the maximum value in (a) and the mean value in (b).

In summary, we designed the frequency-resolved photon-electron spectroscopy to detect the population on the excited states for atoms under impact of the strong laser pulse. With the numerical simulation, we showed the typical FRPE spectrum with two main features for helium, and explained their physical origins. With the spectrum, we presented the detailed scheme to reconstruct population, and validated the scheme with Helium as the example. The current scheme shows a good agreement between reconstructed value and the exact value. However, to experimentally demonstrate the Fourier transform, it's important to establish the phase stability between two pulses. Currently, the stable phase between different color pulses in the experiment [36, 37, 44] have been achieved for weak fields.

REFERENCES

1. P. Agostini, F. Fabre, G. Mainfray, G. Petite, and N. K. Rahman, Phys. Rev. Lett. **42**, 1127 (1979).
2. P. B. Corkum, Phys. Rev. Lett. **71**, 1994 (1993).
3. R. Pazourek, S. Nagele, and J. Burgdörfer, Rev. Mod. Phys. **87**, 765 (2015).
4. M. Sabbar, H. Timmers, Y. J. Chen, A. K. Pymer, Z. H. Loh, S. G. Sayres, S. Pabst, R. Santra, and S. R. Leone, Nat. Phys. **13**, 472 (2017).
5. M. Isinger, R. J. Squibb, D. Busto, S. Zhong, A. Harth, D. Kroon, S. Nandi, C. L. Arnold, M. Miranda, J. M. Dahlström, E. Lindroth, R. Feifel, M. Gisselbrecht, and A. L'Huillier, Science, **358**, 893 (2017).
6. W. Becker, X. Liu, P. J. Ho, and J. H. Eberly, Rev. Mod. Phys. **84**, 1011 (2012).
7. A. McPherson, G. Gibson, H. Jara, U. Johann, T. S. Luk, I. A. McIntyre, K. Boyer, and C. K. Rhodes, J. Opt. Soc. Am. B **4**, 595 (1987).
8. M. Ferray, A. L'Huillier, X. F. Li, L. A. Lompré, G. Mainfray, and C. Manus, J. Phys. B **21**, L31 (1988).
9. M. V Frolov, N. L. Manakov, A. A. Minina, N. V Vvedenskii, A. A. Silaev, M. Y. Ivanov, and A. F. Starace, Phys. Rev. Lett. **120**, 263203 (2018).
10. T. Nubbemeyer, K. Gorling, A. Saenz, U. Eichmann, and W. Sandner, Phys. Rev. Lett. **101**, 233001 (2008).
11. M. P. De Boer and H. G. Muller, Phys. Rev. Lett. **68**, 2747 (1992).
12. H. Zimmermann, J. Buller, S. Eilzer, and U. Eichmann, Phys. Rev. Lett. **114**, 123003 (2015).
13. D. B. Milošević, G. G. Paulus, D. Bauer, and W. Becker, J. Phys. B **39**, R203 (2006).
14. M. Wickenhauser, X. M. Tong, and C. D. Lin, Phys. Rev. A **73**, 011401 (2006).
15. M. Lewenstein, P. Balcou, M. Y. Ivanov, A. L'huillier, and P. Corkum, Phys. Rev. A **49**, 2117 (1994).
16. W. Becker, A. Lohr and M. Kleber, J. Phys. B **27**, L325 (1994).
17. A. Lohr, M. Kleber, R. Kopold, and W. Becker, Phys. Rev. A **55**, R4003 (1997).
18. W. Becker, F. Grasbon, R. Kopold, D. B. Milošević, G. G. Paulus, and H. Walther, Adv. At. Mol. Opt. Phys. **48**, 35 (2002).
19. D. B. Milošević, W. Becker, M. Okunishi, G. Prümper, K. Shimada, and K. Ueda, J. Phys. B **43**, 015401 (2009).
20. R. R. Freeman, P. H. Bucksbaum, H. Milchberg, S. Darack, D. Schumacher, and M. E. Geusic, Phys. Rev. Lett. **59**, 1092 (1987).
21. M. Fushitani, C. N. Liu, A. Matsuda, T. Endo, Y. Toida, M. Nagasono, T. Togashi, M. Yabashi, T. Ishikawa, Y. Hikosaka, T. Morishita, and A. Hishikawa, Nat. Photonics **10**, 102 (2016).
22. W. H. Xiong, L. Y. Peng, and Q. Gong, J. Phys. B At. Mol. Opt. Phys. **50**, 032001 (2017).
23. H. Zimmermann, S. Meise, A. Khujakulov, A. Magaña, A. Saenz, and U. Eichmann, Phys. Rev. Lett. **120**, 123202 (2018).
24. E. P. Power, A. M. March, F. Catoire, E. Sistrunk, K. Krushelnick, P. Agostini, and L. F. DiMauro, Nat. Photonics **4**, 352 (2010).
25. P. C. Li, Y. L. Sheu, C. Laughlin, and S. I. Chu, Nat. Commun. **6**, 7178 (2015).
26. M. T. Hassan, T. T. Luu, A. Moulet, O. Raskazovskaya, P. Zhokhov, M. Garg, N. Karpowicz, A. M. Zheltikov, V. Pervak, F. Krausz, and E. Goulielmakis, Nature **530**, 66 (2016).
27. F. Krausz and M. Ivanov, Rev. Mod. Phys. **81**, 163 (2009).
28. B. K. McFarland, J. P. Farrell, S. Miyabe, F. Tarantelli, A. Aguilar, N. Berrah, C. Bostedt, J. D. Bozek, P. H. Bucksbaum, J. C. Castagna, R. N. Coffee, J. P. Cryan, L. Fang, R. Feifel, K. J. Gaffney, J. M. Glownia, T. J. Martinez, M. Mucke, B. Murphy, A. Natan, T. Osipov, V. S. Petrović, S. Schorb, Th. Schultz, L. S. Spector, M. Swiggers, I. Tenney, S. Wang, J. L. White, W. White, and M. Gühr, Nat. Commun. **5**, 4235 (2014).
29. D. M. Villeneuve, P. Hockett, M. J. J. Vrakking, and H. Niikura, Science **356**, 1150 (2017).
30. Y. Zhang, T. M. Yan, and Y. H. Jiang, Phys. Rev. Lett. **121**, 113201 (2018).
31. M. He, Y. Li, Y. Zhou, M. Li, W. Cao, and P. Lu, Phys. Rev. Lett. **120**, 133204 (2018).
32. F. Penent, P. Lablanquie, R. I. Hall, M. Žitnik, K. Bučar, S. Stranges, R. Richter, M. Alagia, P. Hammond, and J. G. Lambourne, Phys. Rev. Lett. **86**, 2758 (2001).
33. M. Aeschlimann, T. Brixner, A. Fischer, C. Kramer, P. Melchior, W. Pfeiffer, C. Schneider, C. Strüber, P. Tuchscherer, and D. V. Voronine, Science, **333**, 1723 (2011).
34. P. Hamm and M. Zanni, *Concepts and Methods of 2D Infrared Spectroscopy* (Cambridge University Press, 2011).
35. D. M. Jonas, Annu. Rev. Phys. Chem. **54**, 425-463 (2003).
36. T. Oliver, N. Lewis, and G. Fleming, Proc. Natl. Acad. Sci. U. S. A. **111**, 10061 (2014).
37. H. Dong, N. Lewis, T. Oliver, and G. Fleming, J. Chem. Phys. **142**, 174201 (2015).

38. S. L. Sorensen, O. Björneholm, I. Hjelte, T. Kihlgren, G. Öhrwall, S. Sundin, S. Svensson, S. Buil, D. Descamps, A. L'Huillier, J. Norin, and C. G. Wahlström, J. Chem. Phys. **112**, 8038 (2000).
39. A. Stolow, A. E. Bragg, and D. M. Neumark, Chem. Rev. **104**, 1719 (2004).
40. T. Frohnmeyer and T. Baumert, Appl. Phys. B **71**, 259 (2000).
41. J. H. Eberly, Phys. Rev. A **42**, 5750 (1990).
42. M. Feit, J. Fleck, and A. Steiger, J. Comput. Phys. **47**, 412 (1982).
43. X. M. Tong, K. Hino, and N. Toshima, Phys. Rev. A **74**, 031405 (2006).
44. A. Konar, R. Sechrist, Y. Song, V. R. Policht, P. D. Laible, D. F. Bocian, D. Holten, C. Kirmaier, and J. P. Ogilvie, J. Phys. Chem. Lett. **9**, 5219 (2018).

FULL REFERENCES

1. P. Agostini, F. Fabre, G. Mainfray, G. Petite, and N. K. Rahman, "Free-Free Transitions Following Six-Photon Ionization of Xenon Atoms," Phys. Rev. Lett. **42**, 1127 (1979).
2. P. B. Corkum, "Plasma Perspective on Strong-Field Multiphoton Ionization," Phys. Rev. Lett. **71**, 1994 (1993).
3. R. Pazourek, S. Nagele, and J. Burgdörfer, "Attosecond chronoscopy of photoemission," Rev. Mod. Phys. **87**, 765 (2015).
4. M. Sabbar, H. Timmers, Y. J. Chen, A. K. Pymer, Z. H. Loh, S. G. Sayres, S. Pabst, R. Santra, and S. R. Leone, "State-resolved attosecond reversible and irreversible dynamics in strong optical field," Nat. Phys. **13**, 472 (2017).
5. M. Isinger, R. J. Squibb, D. Busto, S. Zhong, A. Harth, D. Kroon, S. Nandi, C. L. Arnold, M. Miranda, J. M. Dahlström, E. Lindroth, R. Feifel, M. Gisselbrecht, and A. L'Huillier, "Photoionization in the time and frequency domain," Science, **358**, 893 (2017).
6. W. Becker, X. Liu, P. J. Ho, and J. H. Eberly, "Theoriesof photoelectron correlation in laser-driven multipleatomicionization," Rev. Mod. Phys. **84**, 1011 (2012).
7. A. McPherson, G. Gibson, H. Jara, U. Johann, T. S. Luk, I. A. McIntyre, K. Boyer, and C. K. Rhodes, "Studies of multiphoton production of vacuum-ultraviolet radiation in the rare gases," J. Opt. Soc. Am. B **4**, 595 (1987).
8. M. Ferray, A. L'Huillier, X. F. Li, L. A. Lompré, G. Mainfray, and C. Manus, "Multiple-harmonic conversion of 1064 nm radiation in rare gases," J. Phys. B **21**, L31 (1988).
9. M. V Frolov, N. L. Manakov, A. A. Minina, N. V Vvedenskii, A. A. Silaev, M. Y. Ivanov, and A. F. Starace, "Control of Harmonic Generation by the Time Delay Between Two-Color, Bicircular Few-Cycle Mid-IR Laser Pulses," Phys. Rev. Lett. **120**, 263203 (2018).
10. T. Nubbemeyer, K. Gorling, A. Saenz, U. Eichmann, and W. Sandner, "Strong-Field Tunneling without Ionization," Phys. Rev. Lett. **101**, 233001 (2008).
11. M. P. De Boer and H. G. Muller, "Observation of Large Populations in Excited States after Short-Pulse Multiphoton Ionization," Phys. Rev. Lett. **68**, 2747 (1992).
12. H. Zimmermann, J. Buller, S. Eilzer, and U. Eichmann, "Strong-Field Excitation of Helium: Bound State Distribution and Spin Effects," Phys. Rev. Lett. **114**, 123003 (2015).
13. D. B. Milošević, G. G. Paulus, D. Bauer, and W. Becker, "Above-threshold ionization by few-cycle pulses," J. Phys. B **39**, R203 (2006).
14. M. Wickenhauser, X. M. Tong, and C. D. Lin, "Laser-induced substructures in above-threshold-ionization spectra from intense few-cycle laser pulses," Phys. Rev. A **73**, 011401 (2006).
15. M. Lewenstein, P. Balcou, M. Y. Ivanov, A. L'huillier, and P. Corkum, "Theory of high-harmonic generation by low-frequency laser fields," Phys. Rev. A **49**, 2117 (1994).
16. W. Becker, A. Lohr and M. Kleber, "Effects of rescattering on above-threshold ionization," J. Phys. B **27**, L325 (1994).
17. A. Lohr, M. Kleber, R. Kopold, and W. Becker, "Above-threshold ionization in the tunneling regime," Phys. Rev. A **55**, R4003 (1997).
18. W. Becker, F. Grasbon, R. Kopold, D. B. Milošević, G. G. Paulus, and H. Walther, "Above-Threshold Ionization: From Classical Features to Quantum Effects," Adv. At. Mol. Opt. Phys. **48**, 35 (2002).
19. D. B. Milošević, W. Becker, M. Okunishi, G. Prümper, K. Shimada, and K. Ueda, "Strong-field electron spectra of rare-gas atoms in the rescattering regime: enhanced spectral regions and a simulation of the experiment," J. Phys. B **43**, 015401 (2009).
20. R. R. Freeman, P. H. Bucksbaum, H. Milchberg, S. Darack, D. Schumacher, and M. E. Geusic, "Above-Threshold Ionization with Subpicosecond Laser Pulses," Phys. Rev. Lett. **59**, 1092 (1987).
21. M. Fushitani, C. N. Liu, A. Matsuda, T. Endo, Y. Toida, M. Nagasono, T. Togashi, M. Yabashi, T. Ishikawa, Y. Hikosaka, T. Morishita, and A. Hishikawa, "Femtosecond two-photon Rabi oscillations in excited He driven by ultrashort intense laser field," Nat. Photonics **10**, 102 (2016).
22. W. H. Xiong, L. Y. Peng, and Q. Gong, "Recent progress of below-threshold harmonic generation," J. Phys. B At. Mol. Opt. Phys. **50**, 032001 (2017).
23. H. Zimmermann, S. Meise, A. Khujakulov, A. Magaña, A. Saenz, and

U. Eichmann, "Limit on Excitation and Stabilization of Atoms in Intense Optical Laser Fields," Phys. Rev. Lett. **120**, 123202 (2018).

24. E. P. Power, A. M. March, F. Catoire, E. Sistrunk, K. Krushelnick, P. Agostini, and L. F. DiMauro, "XFROG phase measurement of threshold harmonics in a Keldysh-scaled system," Nat. Photonics **4**, 352 (2010).

25. P. C. Li, Y. L. Sheu, C. Laughlin, and S. I. Chu, "Dynamical origin of near- and below-threshold harmonic generation of Cs in an intense mid-infrared laser field," Nat. Commun. **6**, 7178 (2015).

26. M. T. Hassan, T. T. Luu, A. Moulet, O. Raskazovskaya, P. Zhokhov, M. Garg, N. Karpowicz, A. M. Zheltikov, V. Pervak, F. Krausz, and E. Goulielmakis, "Optical attosecond pulses and tracking the nonlinear response of bound electrons," Nature **530**, 66 (2016).

27. F. Krausz and M. Ivanov, "Attosecond physics," Rev. Mod. Phys. **81**, 163 (2009).

28. B. K. McFarland, J. P. Farrell, S. Miyabe, F. Tarantelli, A. Aguilar, N. Berrah, C. Bostedt, J. D. Bozek, P. H. Bucksbaum, J. C. Castagna, R. N. Coffee, J. P. Cryan, L. Fang, R. Feifel, K. J. Gaffney, J. M. Glownia, T. J. Martinez, M. Mucke, B. Murphy, A. Natan, T. Osipov, V. S. Petrović, S. Schorb, Th. Schultz, L. S. Spector, M. Swiggers, I. Tenney, S. Wang, J. L. White, W. White, and M. Gühr, "Ultrafast X-ray Auger probing of photoexcited molecular dynamics," Nat. Commun. **5**, 4235 (2014).

29. D. M. Villeneuve, P. Hockett, M. J. J. Vrakking, and H. Niikura, "Coherent imaging of an attosecond electron wave packet," Science **356**, 1150 (2017).

30. Y. Zhang, T. M. Yan, and Y. H. Jiang, "Ultrafast Mapping of Coherent Dynamics and Density Matrix Reconstruction in a Terahertz-Assisted Laser Field," Phys. Rev. Lett. **121**, 113201 (2018).

31. M. He, Y. Li, Y. Zhou, M. Li, W. Cao, and P. Lu, "Direct Visualization of Valence Electron Motion Using Strong-Field Photoelectron Holography," Phys. Rev. Lett. **120**, 133204 (2018).

32. F. Penent, P. Lablanquie, R. I. Hall, M. Žitnik, K. Bučar, S. Stranges, R. Richter, M. Alagia, P. Hammond, and J. G. Lambourne, "Observation of Triplet Doubly Excited States in Single Photon Excitation from Ground State Helium," Phys. Rev. Lett. **86**, 2758 (2001).

33. M. Aeschlimann, T. Brixner, A. Fischer, C. Kramer, P. Melchior, W. Pfeiffer, C. Schneider, C. Strüber, P. Tuchscherer, and D. V. Voronine, "Coherent Two-Dimensional Nanoscopy," Science, **333**, 1723 (2011).

34. P. Hamm and M. Zanni, *Concepts and Methods of 2D Infrared Spectroscopy* (Cambridge University Press, 2011).

35. D. M. Jonas, "Two-dimensional femtosecond spectroscopy," Annu. Rev. Phys. Chem. **54**, 425-463 (2003).

36. T. Oliver, N. Lewis, and G. Fleming, "Correlating the motion of electrons and nuclei with two-dimensional electronic-vibrational spectroscopy," Proc. Natl. Acad. Sci. U. S. A. **111**, 10061 (2014).

37. H. Dong, N. Lewis, T. Oliver, and G. Fleming, "Determining the static electronic and vibrational energy correlations via two-dimensional electronic-vibrational spectroscopy," J. Chem. Phys. **142**, 174201 (2015).

38. S. L. Sorensen, O. Björneholm, I. Hjelte, T. Kihlgren, G. Öhrwall, S. Sundin, S. Svensson, S. Buil, D. Descamps, A. L'Huillier, J. Norin, and C. G. Wahlström, "Femtosecond pump-probe photoelectron spectroscopy of predissociative Rydberg states in acetylene," J. Chem. Phys. **112**, 8038 (2000).

39. A. Stolow, A. E. Bragg, and D. M. Neumark, "Femtosecond Time-Resolved Photoelectron Spectroscopy," Chem. Rev. **104**, 1719 (2004).

40. T. Frohnmeyer and T. Baumert, "Femtosecond pump-probe photoelectron spectroscopy on Na_2: a tool to study basic coherent control schemes," Appl. Phys. B **71**, 259 (2000).

41. J. H. Eberly, "Scale variation in a one-dimensional model of an atom interacting with a strong laser field" Phys. Rev. A **42**, 5750 (1990).

42. M. Feit, J. Fleck, and A. Steiger, "Solution of the Schröedinger equation by a spectral method," J. Comput. Phys. **47**, 412 (1982).

43. X. M. Tong, K. Hino, and N. Toshima, "Phase-dependent atomic ionization in few-cycle intense laser fields," Phys. Rev. A **74**, 031405 (2006).

44. A. Konar, R. Sechrist, Y. Song, V. R. Policht, P. D. Laible, D. F. Bocian, D. Holten , C. Kirmaier, and J. P. Ogilvie, "Electronic Interactions in the Bacterial Reaction Center Revealed by Two-Color 2D Electronic Spectroscopy," J. Phys. Chem. Lett. **9**, 5219 (2018).